

Vibration–rotational Spectra of GaF and Molecular Properties of Diatomic Fluorides of Elements in Group 13

J. F. Ogilvie*

Academia Sinica, Institute of Atomic and Molecular Sciences, P.O. Box 23-166, Taipei 10 764, Taiwan

Hirohichi Uehara and Kouji Horiai

Department of Chemistry, Faculty of Science, Josai University, Keyakidai, Sakado, Saitomo 350-02, Japan

From new measurements of vibration–rotational spectra of $^{69}\text{Ga}^{19}\text{F}$ and $^{71}\text{Ga}^{19}\text{F}$ in absorption with laser diodes in the wavenumber region $54\,800 \leq \bar{\nu}/\text{m}^{-1} \leq 63\,800$, we evaluated radial coefficients that serve to reproduce the wavenumbers of 229 IR lines and published frequencies of 27 microwave lines within small uncertainties. The maximum range of validity of radial functions is $1.57 \leq R/10^{-10} \text{ m} \leq 2.10$, and $R_e = (1.774\,341\,0 \pm 0.000\,001\,5) \times 10^{-10} \text{ m}$, after corrections for non-adiabatic effects. For comparison with results of GaF and of TlF previously reported, we analysed published microwave and IR spectra of BF, AlF and InF; maximum ranges of validity of pertinent radial functions and a table of parameters are presented. For BF we find experimental evidence for the sense $-\text{BF}^+$ of electric polarity.

Discrete diatomic molecules containing fluorine as one atomic centre have diverse chemical properties because the electronic binding can vary from strongly covalent to essentially ionic. These chemical properties reflect the physical properties that one deduces from analyses of various spectra of these diatomic molecules in the gaseous phase. The chemical and physical significance of spectral parameters depends on the extent of the spectra. An early analysis of many bands of the same molecular species was provided in work on HF by Thrush and co-workers.¹ Just as instruments to measure IR spectra under conditions of increasingly high resolution and precision became available during the past several decades, theoretical formalisms have been concurrently developed to match a need to reproduce spectral data by means of few chemically and physically meaningful parameters for the numerous spectral data;² the latter comprise frequencies of lines in the microwave region and wavenumbers of lines in the IR region that characterise transitions between vibration–rotational states within a single electronic state.

In the present work we measured absorption spectra of GaF molecules in the gaseous phase near 730 K and undertook a global analysis of all available data of suitable precision, combining our new vibration–rotational measurements in the IR region with published frequencies of pure rotational transitions in the microwave region. Thereby we evaluated coefficients of radial functions that pertain to potential energy and related properties according to a conventional treatment of separate electronic and nuclear motions.^{3,4} In this analysis we included auxiliary information about electric and magnetic properties so as to ensure that all parameters possess maximum chemical and physical significance. From analysis of similar spectral data of other diatomic fluorides of elements of Group 13 of the periodic table, we present a comparison of parameters of GaF with those of BF, AlF, InF and TlF, all evaluated according to the same protocol.

Experimental

We measured spectra of GaF in absorption using a spectrometer (Spectra-Physics, Laser Photonics, SP5000) having a laser diode as source and a high-temperature White cell with a resonator of length 1 m.⁵ The White cell contained multiply reflecting mirrors plated with gold and mounted at both ends of a stainless-steel pipe of external diameter 80 mm. The

central portion of the pipe was heated with an electric furnace; the mirror mounts were thermally insulated from the heated zone by water cooling the body of the cell near the ends of the heated zone of the pipe. The inner wall of the pipe was lined with a stainless-steel mesh wick. For 20 traversals within the cell the length of the optical path was 20 m. The mirrors and their mounts of this White cell were those detached from a commercial cell with a long absorbing path (Spectra-Physics, LO-3-2). As these mirrors had dovetailing chevrons ground into their backs, their removal to clean deteriorated surfaces and replacement in their mounts was easily done without altering the alignment.

We charged the White cell with a mixture of GaF₃ (10 g) and metallic Ga (15 g) and generated gaseous GaF in the presence of other species by heating the cell to *ca.* 730 K. A buffer gas, argon at a pressure 1070 Pa, suppressed migration of sample gas from the heated zone of the cell.

Optical reflections within the cell unavoidably produced fringes. As processing with Fourier transformations eliminated simultaneously both these fringes and high-frequency noise,^{5–7} large time coefficients were not required for phase-sensitive detection to observe signals.⁷ The full sweep, of width typically 70 m^{-1} , required 23 s with a time coefficient 10 ms, the smallest practicable in our spectrometer.

This spectrometer was equipped with two photoconductive detectors of germanium doped with copper and cooled with liquid helium. We calibrated the wavenumbers of spectral lines of GaF with reference spectra of CO₂,⁸ N₂O⁸ and SO₂ (J. W. C. Johns, personal communication to H.U., 1987); we measured the differences between the wavelength of a standard line and a line of GaF with a newly constructed confocal etalon of path 45 cm in air, with a free spectral range 1.11 m^{-1} . The spacer that forms the structure to support the etalon was a silica tube of outer diameter 30 mm, both ends of which were fitted with windows of thallium bromiodide (KRS-5) of thickness 3 mm; their inner surfaces were coated with gold in a thin layer to provide a finesse about six. For measurements of each set within a particular spectral range, the procedure consisted of four successive scans of reference gas, GaF, GaF plus reference gas, and etalon. Thereby the speed of scanning in these experiments, much greater than formerly, both enabled efficient measurements and eliminated uncertainty that temporal variation of the starting point of a sweep in each of four successive scans might introduce.

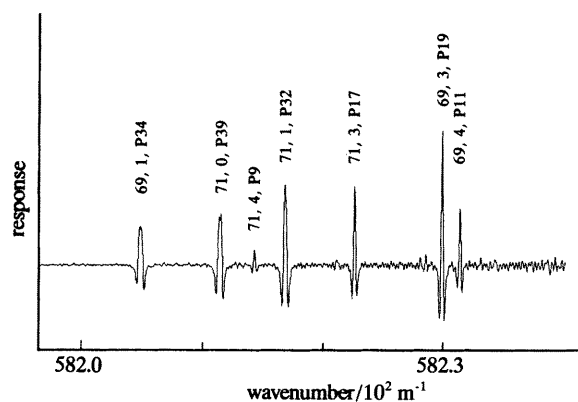


Fig. 1 Portion of the IR spectrum of gaseous GaF in the region $58\,200 < \tilde{\nu}/\text{m}^{-1} < 58\,245$; characters above the signals indicate the isotopic variant (69 for $^{69}\text{Ga}^{19}\text{F}$ and 71 for $^{71}\text{Ga}^{19}\text{F}$), the quantum number ν of the vibrational state of smaller energy (in the sequence with $\Delta\nu = 1$), and the quantum number J of the rotational state in vibrational state ν from which the transition occurred in the P branch. Fringes of period 0.25 m^{-1} appear in the range $58\,215 < \tilde{\nu}/\text{m}^{-1} < 58\,242$. The response is the second derivative of the absorption; relative intensities are inaccurate because the intensity of light from a laser diode varied with wavenumber and because absorption was not normalised.

The length of absorbing path of sample enabled signals to be observed with GaF at a small partial pressure and a temperature 730 K. Within overlapping bands of GaF with $\Delta\nu = 1$, spectral lines with narrow widths, because of this small partial pressure of the sample, were measured with a satisfactory ratio of signal to noise in the range of wavenumber $54\,800 < \tilde{\nu}/\text{m}^{-1} < 63\,800$. A portion of the observed spectrum of GaF in Fig. 1, with assignments, illustrates the quality of our spectra.

Processing of Measured Spectra by Fourier Transformation

We transferred the digitised spectra to a microcomputer (NEC PC-H98 model 100) with which we processed all spectra by Fourier transformation with programs in FORTRAN and BASIC.^{5,6} Dominant parts of fringes were those spaced at 0.25 m^{-1} indicating the effect of an etalon of length 2 m. A typical example of fringes, much weaker than most signals of GaF, is discernible in Fig. 1.

The fringes and noise of large frequency were eliminated on multiplying by the weighting function the array in Fourier space that was obtained on Fourier transformation of the observed spectrum; this spectrum in each full sweep consisted of an array of length 2048 data. We used generally rectangular (occasionally trapezoidal) functions for truncation.⁷ The period of fringes spaced at 0.25 m^{-1} was equivalent to six points in the original data array; the spectral resolution of GaF was equivalent to eight points, which correspond to the width at zero crossings of a line having the shape of a second derivative. According to a criterion⁵ to truncate a Fourier space array we thus selected a boundary larger than 256 ($=2048/8$), thus significantly smaller than 341 ($=2048/6$) points corresponding to the signal in the Fourier domain of fringes spaced at 0.25 m^{-1} .

To determine the wavenumbers of spectral lines, we fitted, according to the criterion of least squares, a quadratic curve to data points about each line at the position obtained on Fourier transformation.

Assignment of Spectral Lines

First we predicted vibration-rotational transitions in progressions of $^{69}\text{Ga}^{19}\text{F}$ and $^{71}\text{Ga}^{19}\text{F}$ with $\Delta\nu = 1$ and

$0 \leq \nu \leq 2$ by means of rotational parameters from microwave spectra⁹ and vibrational parameters from vibration-rotational spectra in emission recorded at a resolution 10 m^{-1} .¹⁰ As these parameters were accurate, we located intense lines at wavenumbers near predicted values. Then we began the analysis of combined microwave and IR spectral data with a computer program RADIATOM² and extended predictions as far as necessary. According to this method most lines of significant intensity within ranges in which the laser diode operated were assigned satisfactorily. Thus in the IR region 115 lines of $^{69}\text{Ga}^{19}\text{F}$ in the range up to $\nu = 8$ and $J = 83$ and 114 lines of $^{71}\text{Ga}^{19}\text{F}$ in the range up to $\nu = 8$ and $J = 74$ and in the microwave region⁹ 13 lines of $^{69}\text{Ga}^{19}\text{F}$ and 14 lines of $^{71}\text{Ga}^{19}\text{F}$ comprised our final input data; the set numbers 256 transitions. Multiple spectral scans of some lines indicated that the reproducibility of IR measurements was within $\pm 0.05\text{ m}^{-1}$ relative to standard lines. Based on assessment of various experimental factors, the uncertainty of most lines we set to be 0.05 m^{-1} . The eventual standard deviation of the fit of IR lines was about 0.05 m^{-1} ; magnitudes of residuals of microwave lines in the combined fit were generally smaller than their nominal uncertainties specified by the original authors.⁹ A list of assigned lines in our IR absorption spectrum of $^{69}\text{Ga}^{19}\text{F}$ appears in Table 1 with their residuals in the final fit, and of lines of $^{71}\text{Ga}^{19}\text{F}$ similarly in Table 2.

Reduction of Assigned Spectra to Radial Coefficients

As the basis of a common quantitative treatment of spectra of all diatomic fluorides of elements of Group 13, we adopted an effective Hamiltonian for nuclear motion of the form⁴

$$\mathcal{H}_{\text{eff}} = \hat{P}[1 + \beta(R)]\hat{P}/2\mu + V(R) + V'(R) + hcB_e[1 + \alpha(R)](J^2 + J)R_e^2/R^2 \quad (1)$$

Here R denotes the internuclear separation and R_e its value at the minimum of internuclear potential energy $V(R)$, μ the reduced mass, $B_e \equiv h/(8\pi^2c\mu R_e^2)$ the equilibrium rotational parameter, and \hat{P} the operator for linear momentum of the nuclei. To apply this Hamiltonian we transformed to the variable for reduced displacement

$$z \equiv 2(R - R_e)/(R + R_e) \quad (2)$$

that remains finite throughout the range of molecular existence: for $0 \leq R < \infty$, $-2 \leq z < 2$.^{11,12} Henceforth with SI units of wavenumber¹³ for appropriate quantities, we represent the potential energy $V(R)$ formally independent of nuclear mass in the form¹¹

$$V(z) = c_0 z^2 \left(1 + \sum_{j=1} c_j z^j \right) \quad (3)$$

For an assumed diatomic molecule AB having nuclei a and b with protons of unequal number, further functions dependent on individual nuclear masses M_a and M_b include those for non-adiabatic vibrational effects,¹⁴ whereby electrons follow nuclei imperfectly during oscillations of the latter with respect to the centre of mass,

$$\beta(R) = \beta^a(R) + \beta^b(R) \rightarrow m_e \left(\sum_{j=0} s_j^a z^j / M_a + \sum_{j=0} s_j^b z^j / M_b \right) \quad (4)$$

for non-adiabatic rotational effects,¹⁴ whereby electrons follow nuclei imperfectly during rotation of the latter about the centre of mass,

$$\alpha(R) = \alpha^a(R) + \alpha^b(R) \rightarrow m_e \left(\sum_{j=0} t_j^a z^j / M_a + \sum_{j=0} t_j^b z^j / M_b \right) \quad (5)$$

Table 1 Assignments of vibration-rotational transitions of $^{69}\text{Ga}^{19}\text{F}$ measured with a diode laser^a

line	$\tilde{\nu}/\text{m}^{-1}$	$\delta\tilde{\nu}/\text{m}^{-1}$	line	$\tilde{\nu}/\text{m}^{-1}$	$\delta\tilde{\nu}/\text{m}^{-1}$
$^{69}\text{Ga}^{19}\text{F } v' = 1 \leftarrow v'' = 0$					
P(61)	56 214.55	0.01	R(0)	61 650.12	-0.03
P(51)	57 227.55	-0.01	R(5)	61 996.82	0
P(44)	57 906.62	0.03	R(6)	62 064.52	0.10
P(37)	58 560.34	-0.01	R(15)	62 646.84	-0.01
P(13)	60 604.11	-0.02	R(16)	62 708.52	-0.11
P(8)	60 990.39	0.06	R(28)	63 404.03	0.05
P(3)	61 362.51	-0.03	R(34)	63 719.29	-0.01
$^{69}\text{Ga}^{19}\text{F } v' = 2 \leftarrow v'' = 1$					
P(68)	54 874.17	-0.05	P(4)	60 641.93	0.07
P(55)	56 215.94	-0.04	R(5)	61 343.84	0.02
P(48)	56 903.63*	-0.21	R(9)	61 608.65	-0.02
P(34)	58 204.61	-0.03	R(10)	61 673.47	0.03
P(30)	58 557.59	0.01	R(15)	61 988.65	0.02
P(26)	58 902.03	-0.02	R(17)	62 110.68	0.05
P(22)	59 237.99	0.01	R(27)	62 685.38	-0.01
P(18)	59 565.28	0	R(41)	63 389.69	0.01
P(17)	59 645.88	0.12	R(49)	63 738.59	0.02
P(8)	60 345.29	-0.04			
$^{69}\text{Ga}^{19}\text{F } v' = 3 \leftarrow v'' = 2$					
P(62)	54 904.14	0	R(20)	61 636.09	0
P(59)	55 209.87	-0.04	R(21)	61 693.97	-0.01
P(42)	56 858.64	0.02	R(26)	61 974.71	0.09
P(38)	57 225.34	-0.02	R(27)	62 029.03	0.04
P(34)	57 583.89	0.04	R(28)	62 082.77	0.02
P(14)	59 249.93	0.01	R(40)	62 681.38	-0.05
P(10)	59 557.31	0	R(48)	63 032.33	0.10
P(9)	59 632.83	0.04	R(58)	63 415.43	0.03
P(5)	59 929.21	0.02	R(67)	63 706.97	0.05
R(4)	60 631.22	0.05	R(68)	63 736.17	0.01
R(9)	60 961.00	0.01	R(69)	63 764.68	-0.09
R(15)	61 337.96	0.06			
$^{69}\text{Ga}^{19}\text{F } v' = 4 \leftarrow v'' = 3$					
P(56)	54 913.94	0.01	R(9)	60 320.65	-0.04
P(53)	55 208.53	-0.02	R(14)	60 633.62	-0.06
P(46)	55 879.79	0.06	R(26)	61 326.11	0.01
P(35)	56 882.02	-0.07	R(32)	61 640.76	0.02
P(31)	57 231.66	0.07	R(33)	61 691.10	-0.02
P(27)	57 572.79	0.02	R(39)	61 980.90	0.05
P(23)	57 905.58	0.03	R(40)	62 027.06	0.03
P(19)	58 229.87	0.01	R(41)	62 072.68	0.05
P(15)	58 545.54	-0.08	R(42)	62 117.62	0
P(6)	59 224.36	-0.06	R(56)	62 683.59	-0.04
P(1)	59 582.34	0	R(66)	63 013.93	-0.02
R(3)	59 926.37	-0.01	R(82)	63 411.49	-0.01
$^{69}\text{Ga}^{19}\text{F } v' = 5 \leftarrow v'' = 4$					
P(50)	54 903.76	0	R(8)	59 624.03	0.17
P(28)	56 877.68	0.03	R(13)	59 937.26	0.10
P(24)	57 209.92	0.01	R(25)	60 630.81	-0.03
P(20)	57 533.82	0.04	R(39)	61 334.28	0.08
P(11)	58 231.41	0.01	R(46)	61 642.28	0.03
P(2)	58 885.27	-0.01	R(55)	61 994.87	0.05
R(2)	59 229.29	-0.05	R(56)	62 031.06	0.11
R(7)	59 559.53	0.02	R(78)	62 668.76	0.01
$^{69}\text{Ga}^{19}\text{F } v' = 6 \leftarrow v'' = 5$					
P(21)	56 845.47	0	R(37)	60 602.05	-0.18
P(12)	57 542.40	0.05	R(45)	60 958.43	0.01
P(7)	57 910.83	-0.01	R(55)	61 349.77	-0.01
R(6)	58 870.33	0.07	R(77)	61 995.33	-0.02
R(12)	59 248.24	0			
$^{69}\text{Ga}^{19}\text{F } v' = 7 \leftarrow v'' = 6$					
P(21)	56 244.24	-0.03	R(0)	57 858.29	0.13
P(17)	56 556.75	-0.05	R(11)	58 566.80	-0.02
P(13)	56 860.91	-0.03	R(45)	60 323.91	-0.08
$^{69}\text{Ga}^{19}\text{F } v' = 8 \leftarrow v'' = 7$					
P(18)	55 883.19	-0.05	R(28)	58 907.95	-0.04
R(10)	57 892.86	0.05	R(42)	59 569.68	-0.03

Table 2 Assignments of vibration-rotational transitions of $^{71}\text{Ga}^{19}\text{F}$ measured with a diode laser^a

line	$\tilde{\nu}/\text{m}^{-1}$	$\delta\tilde{\nu}/\text{m}^{-1}$	line	$\tilde{\nu}/\text{m}^{-1}$	$\delta\tilde{\nu}/\text{m}^{-1}$
$^{71}\text{Ga}^{19}\text{F } v' = 1 \leftarrow v'' = 0$					
P(72)	54 901.09	-0.02	P(1)	61 322.07	-0.02
P(69)	55 224.07	-0.01	R(3)	61 672.36	0.01
P(66)	55 542.77	0.02	R(8)	62 008.38	-0.03
P(63)	55 857.08	0.01	R(9)	62 073.99	0.09
P(53)	56 872.98	-0.01	R(19)	62 696.99	-0.06
P(46)	57 554.45	-0.01	R(25)	63 042.96	0.06
P(39)	58 211.00	-0.02	R(32)	63 419.57	0.16
P(14)	60 346.00	0.04	R(38)	63 718.68	-0.07
P(6)	60 957.74	-0.03	R(39)	63 766.39	-0.13
$^{71}\text{Ga}^{19}\text{F } v' = 2 \leftarrow v'' = 1$					
P(57)	55 865.31	0	P(6)	60 315.36	-0.11
P(50)	56 555.41	0.01	P(2)	60 605.71	-0.02
P(47)	56 843.71	0.02	R(2)	60 956.00	-0.03
P(43)	57 221.03	0.01	R(8)	61 357.74	-0.03
P(39)	57 590.26	0.04	R(12)	61 614.25	0.02
P(36)	57 861.70	-0.02	R(13)	61 676.93	0.01
P(32)	58 216.49	0	R(18)	61 981.72	0.04
P(28)	58 562.87	-0.03	R(30)	62 653.57	-0.04
P(24)	58 900.85	-0.04	R(31)	62 705.69	-0.08
P(20)	59 230.31	-0.06	R(46)	63 416.33	0.08
P(15)	59 630.15	0.01	R(54)	63 739.21	-0.03
$^{71}\text{Ga}^{19}\text{F } v' = 3 \leftarrow v'' = 2$					
P(61)	54 863.16	-0.01	R(12)	60 968.93	-0.01
P(51)	55 853.53	0.01	R(18)	61 333.46	0.04
P(47)	56 235.80	-0.10	R(23)	61 621.31	0
P(40)	56 885.79	0.01	R(30)	61 999.87	0
P(32)	57 598.02	0.04	R(44)	62 670.00	0
P(29)	57 856.52	-0.03	R(53)	63 038.55	0.10
P(12)	59 232.06	-0.03	R(75)	63 728.54	0.03
R(2)	60 315.76	-0.02			
$^{71}\text{Ga}^{19}\text{F } v' = 4 \leftarrow v'' = 3$					
P(55)	54 868.53	-0.01	R(17)	60 633.62	-0.04
P(48)	55 541.02	-0.03	R(23)	60 978.06	0.01
P(37)	56 548.74	-0.01	R(30)	61 353.48	-0.04
P(33)	56 899.83*	-0.22	R(36)	61 652.49	-0.03
P(21)	57 904.37	0	R(37)	61 700.23	-0.06
P(17)	58 222.41	0.04	R(44)	62 018.05	0.01
P(13)	58 531.82	-0.04	R(61)	62 666.59	-0.04
P(8)	58 906.61	-0.03	R(62)	62 699.21	-0.07
R(12)	60 330.94	-0.01	R(73)	63 017.28	-0.11
$^{71}\text{Ga}^{19}\text{F } v' = 5 \leftarrow v'' = 4$					
P(45)	55 226.58	-0.05	R(28)	60 610.84	-0.07
P(38)	55 859.41	-0.01	R(35)	60 962.98	-0.02
P(34)	56 209.95	-0.04	R(43)	61 330.20	0.04
P(30)	56 552.39	-0.03	R(44)	61 373.28	-0.12
P(26)	56 886.68	0.02	R(50)	61 620.23	-0.01
P(22)	57 212.60	-0.02	R(51)	61 659.18	-0.09
P(13)	57 915.33	-0.04	R(52)	61 697.67	-0.04
P(9)	58 213.89	0	R(60)	61 983.37	-0.01
R(10)	59 576.10	-0.01	R(61)	62 016.36	0.02
R(11)	59 638.48	0.06	R(64)	62 111.70	0.14
R(23)	60 341.93	-0.10	R(88)	62 671.81	0.10
$^{71}\text{Ga}^{19}\text{F } v' = 6 \leftarrow v'' = 5$					
P(35)	55 527.69	0	R(27)	59 927.65	-0.01
P(31)	55 869.49	0.02	R(35)	60 329.00	-0.02
P(19)	56 845.82	0.04	R(50)	60 980.70	0
P(5)	57 889.71	0.02	R(60)	61 340.68	0.02
R(9)	58 891.02	-0.06			
$^{71}\text{Ga}^{19}\text{F } v' = 7 \leftarrow v'' = 6$					
P(28)	55 527.30	0.07	P(11)	56 851.25	-0.02
P(24)	55 852.17	-0.01	P(6)	57 211.87	-0.09
P(15)	56 553.34	0.11	R(19)	58 869.60	0.04
$^{71}\text{Ga}^{19}\text{F } v' = 8 \leftarrow v'' = 7$					
P(7)	56 541.62	-0.04	R(7)	57 543.32	0.05
R(2)	57 222.77	-0.06	R(13)	57 909.90	0.10

^a See footnote of Table 1.

^a In Tables 1 and 2, for each designated line in the P or R branch of the specified band of the named isotopic variant, $\tilde{\nu}$ is the measured wavenumber and $\delta\tilde{\nu}$ is the difference between the wavenumber measured and wavenumber calculated with parameters of GaF in Table 3. An asterisk marks the wavenumber of a line that was precluded from influencing the fit.

and for the contribution to the internuclear potential energy dependent on nuclear mass, *i.e.* generally adiabatic effects¹⁴ whereby the potential energy depends not only on the distance between the nuclei but also slightly on their relative momenta,

$$V(R) = V^a(R) + V^b(R) \rightarrow m_e \left(\sum_{j=1}^a u_j^a z^j / M_a + \sum_{j=1}^b u_j^b z^j / M_b \right) \quad (6)$$

As nuclear masses are generally known less accurately than atomic masses and as discrepancies between masses of these kinds have immaterial effects on the ultimate parameters and their interpretation, we employed atomic masses.¹⁵

Discrete molecular energies $\tilde{E}_{v,J}$ within a particular electronic state, or vibration–rotational terms, we express in the form²

$$\tilde{E}_{v,J} = \sum_{k=0} \sum_{l=0} (Y_{kl} + Z_{kl}^{i,a} + Z_{kl}^{i,b} + Z_{kl}^{v,a} + Z_{kl}^{v,b}) \times (v + \frac{1}{2})^k (J^2 + J)^l \quad (7)$$

Differences between these eigenvalues are measured wavenumbers of transitions, $\tilde{\nu} = \tilde{E}_{v',J'} - \tilde{E}_{v'',J''}$. Dependences of term coefficients Y_{kl} and Z_{kl} on equilibrium internuclear separation R_e , equilibrium force coefficient k_e and coefficients in radial functions [eqn. (3)–(6)] are explained elsewhere.² In eqn. (7), that defines energies according to the Hamiltonian in eqn. (1), explicit dependences of $E_{v,J}$, Y_{kl} and various Z_{kl} on a particular isotopic variant are suppressed. To treat adiabatic and non-adiabatic effects, which imply the coupling of electronic and nuclear motions, by means of radial functions of R , which imply the separate treatment of these motions, may appear incongruous; for the electronic ground state and in particular for its vibration–rotational states far from the dissociation limit, the formal interactions with energetically distant, electronically excited states may be sufficiently weak that they can be considered to act as small and homogeneous perturbations.⁴

Even though these adiabatic and non-adiabatic effects are mathematical artifacts, for the reason just stated, experimental information is associated with non-adiabatic effects. The rotation of an otherwise non-magnetic diatomic molecule (in an electronic state $^1\Sigma^+$ or 0^+) induces a small magnetic dipolar moment;¹⁶ the interaction of this molecular moment with an externally applied magnetic field produces splitting of spectral lines according to the Zeeman effect. Proportional to the magnetogyric ratio that is the quotient of induced rotational magnetic dipolar moment and rotational angular momentum, the rotational g factor, or g_J , is a measure of the extent of the splitting, according to M_J , of the energy of a particular vibration–rotational state (for $J > 0$). g_J is thus an expectation value, $\langle vJ | \alpha(R) | vJ \rangle$ or $\langle vJ | g_J(R) | vJ \rangle$, of a particular state denoted by vibrational quantum number v and rotational quantum number J . For a net electrically neutral diatomic molecule of relative polarity $^+AB^-$, we suppose two contributions to the g factor, g_J^{na} attributed to interaction between electronic and nuclear motions, and the other from a rotating electric dipole of moment μ_e (at distance R_e):

$$g_J = g_J^{na} + m_p (M_a^{-1} - M_b^{-1}) \mu_e / (eR_e) \quad (8)$$

in which m_p is the mass of the proton and e its electric charge. The equations to partition the g factor between contributions of the separate atomic centres thus become¹⁷

$$t_a^0 = \mu [g_J / m_p + 2\mu_e / (eR_e M_b)] \quad (9)$$

$$t_b^0 = \mu [g_J / m_p - 2\mu_e / (eR_e M_a)] \quad (10)$$

We postulate radial functions of three kinds beyond mechanical effects within the potential energy $V(z)$,^{2,14} namely functions for adiabatic, non-adiabatic rotational and non-adiabatic vibrational effects of atomic centres of each type; in practice information of at most two kinds can be generally deduced from spectra recorded for samples without externally applied fields, namely the dependence on individual atomic (or nuclear) masses and the extra rotational effects. Measurements of the rotational g factor in varied vibration–rotational states by means of the Zeeman effect provide information that enables in principle separate evaluation of non-adiabatic rotational effects.^{2,14}

In the computer program RADIATOM analytic expressions of term coefficients Y_{kl} and various Z_{kl} that appear in eqn. (7) in terms of their various radial coefficients in eqn. (3)–(6), and expressions also of derivatives of residuals with respect to these radial coefficients, are combined with a procedure for non-linear regression according to a criterion of minimum sum of squares of residuals; hence we undertake to fit wavenumbers of assigned transitions to pertinent radial coefficients in a selected set.² The criterion of the best model is the F statistic,² and a criterion of a successful fit of that model is a satisfactory value of the normalised standard deviation of the fit. Each wavenumber in the data set has an individually assigned uncertainty of measurement; the weight of an item during a fit is the reciprocal square of that uncertainty. Thereby we generate not only estimated standard deviations of adjusted parameters and a matrix of correlation coefficients between those parameters but also values of coefficients U_{kl} in the empirical relation¹⁸

$$\tilde{E}_{v,J} = \sum_{k=0} \sum_{l=0} U_{kl} \mu^{-(k/2+l)} (v + \frac{1}{2})^k (J^2 + J)^l \times [1 + m_e (\Delta_{kl}^a / M_a + \Delta_{kl}^b / M_b)] \quad (11)$$

in which coefficients U_{kl} are related only to the parameters R_e and coefficients c_j , $j \geq 0$, whereas coefficients $\Delta_{kl}^{a,b}$ are related to coefficients in all radial functions (3)–(6); coefficients U_{kl} and $\Delta_{kl}^{a,b}$ are formally independent of mass. This equation serves to define auxiliary parameters $U_{1,0}$ and $U_{0,1}$ that appear in Table 3.

When we applied RADIATOM to vibration–rotational transitions of GaF in Tables 1 and 2, and to complementary microwave data,⁹ the model that produced the maximum value of the F statistic comprised only eight fitted parameters: $U_{1,0}$, $U_{0,1}$ and c_j with $1 \leq k \leq 6$, presented in Table 3. The only other non-zero parameters, $t_a^{0a} = -0.4382 \pm 0.0077$ and $t_b^0 = -1.0131 \pm 0.0030$ constrained during fits, we calculated with eqn. (9) and (10) according to known values of the electric dipolar moment¹⁹ and rotational g factor²⁰ for $^{69}\text{Ga}^{19}\text{F}$ in the state $v = 0$, $J = 1$. By means of these only ten parameters, eight adjusted and two constrained, 256 transitions of $^{69}\text{Ga}^{19}\text{F}$ and $^{71}\text{Ga}^{19}\text{F}$ up to $v = 8$ were fitted collectively; the normalised standard deviation was 0.986 and the F statistic was 9.06×10^{13} . The maximum range of validity of radial functions of GaF in Table 3 is $1.57 \leq R/10^{-10} \text{ m} \leq 2.10$.

We treated similarly pure rotational and vibration–rotational data of the other four diatomic fluorides of elements in Group 13. Data of BF comprise six pure rotational transitions up to $v = 1$ and 100 vibration–rotational transitions up to $v = 3$ and $J = 53$ for $^{10}\text{B}^{19}\text{F}$, 11 pure rotational transitions up to $v = 2$ and 365 vibration–rotational transitions up to $v = 5$ and $J = 62$ for $^{11}\text{B}^{19}\text{F}$.²¹ Uncertainties of many IR lines were set to be 0.03 m^{-1} ,²¹ for a significant fraction of vibration–rotational transitions the uncertainties set larger by the original authors²¹ we re-evaluated during our fitting. In the best model the normalised standard deviation of the fit was 1.086 and the F statistic was 4.73×10^{14} .

Table 3 Coefficients of radial functions and other molecular properties of diatomic fluorides of Group 13 elements in states $X^1\Sigma^+$ or X^0^+ , all independent of nuclear mass; $M = B, Al, Ga, In$ or Tl^a

parameter	BF	AlF	GaF	InF	TlF
c_0/m^{-1}	$32\,398\,736.9 \pm 49.3$	$29\,127\,635.3 \pm 6.5$	$26\,933\,491.7 \pm 17.9$	$27\,314\,122.7 \pm 5.8$	$25\,482\,480.6 \pm 67$
c_1	$-1\,934\,516.2 \pm 0.000\,0148$	$-2\,183\,302.2 \pm 0.000\,0108$	$-2\,298\,462 \pm 0.000\,049$	$-2\,437\,139.2 \pm 0.000\,009\,2$	$-2\,400\,110 \pm 0.000\,036$
c_2	$1\,917\,422 \pm 0.000\,088$	$2\,789\,770 \pm 0.000\,072$	$3\,273\,83 \pm 0.000\,32$	$3\,570\,014 \pm 0.000\,075$	$3\,394\,578 \pm 0.000\,24$
c_3	$-0.955\,36 \pm 0.000\,82$	$-2.219\,77 \pm 0.000\,92$	$-3.143\,2 \pm 0.005\,9$	$-3.520\,33 \pm 0.000\,94$	$-3.397\,9 \pm 0.004\,6$
c_4	$0.482\,7 \pm 0.006\,5$	$0.943\,4 \pm 0.007\,3$	1.442 ± 0.053	$1.870\,5 \pm 0.008\,7$	$2.330\,7 \pm 0.043$
c_5	$-0.407\,7 \pm 0.026\,1$	$-0.980\,3 \pm 0.031$	-0.101 ± 0.156	$-0.160\,9 \pm 0.041$	$1.012\,3 \pm 0.103$
c_6	-2.234 ± 0.130	5.268 ± 0.168	8.72 ± 1.56	4.700 ± 0.199	[0]
r_0^M	$[-1.527\,1]$	$[-0.665\,1]$	$[-0.438\,2]$	$[-0.287]$	$[-0.158\,07]$
r_6^F	$[-1.277\,4]$	$[-1.050\,2]$	$[-1.013\,1]$	$[-1.00]$	$[-0.995\,81]$
r_1^M	2.95 ± 0.83	[0]	[0]	[0]	[0]
$u_1^M/10^6\,m^{-1}$	-5.93 ± 1.45	[0]	[0]	[0]	-508.79 ± 31.4
s_0^M	$1.7578 \pm 0.014\,4$	[0]	[0]	[0]	[0]
$U_{1,0}/m^{-1}\,u^{1/2}$	$370\,167.788 \pm 0.144$	$267\,890.956 \pm 0.041$	$240\,180.378 \pm 0.095$	$216\,162.834 \pm 0.029$	$198\,874.053 \pm 0.067$
$U_{0,1}/m^{-1}\,u$	$1\,057.3266 \pm 0.002\,4$	$615.957\,692 \pm 0.000\,050$	$535.454\,281 \pm 0.000\,067$	$427.675\,927 \pm 0.000\,025$	$388.020\,40 \pm 0.001\,29$
$k_e/N\,m^{-1}$	$807.323\,85 \pm 0.000\,79$	$422.830\,82 \pm 0.000\,28$	$339.879\,98 \pm 0.000\,34$	$275.304\,041 \pm 0.000\,179$	$233.027\,29 \pm 0.000\,21$
$R_e/10^{-10}\,m$	$1.262\,681\,1 \pm 0.000\,001\,8$	$1.654\,332\,6 \pm 0.000\,001\,4$	$1.774\,341\,0 \pm 0.000\,001\,5$	$1.985\,367\,4 \pm 0.000\,001\,7$	$2.084\,351\,7 \pm 0.000\,003\,9$

^a Each specified uncertainty denotes one estimated standard error propagated from input data of frequencies and wavenumbers of assigned lines; errors of k_e and R_e include uncertainties of fundamental constants h and N_A ; brackets enclose values, of which estimated standard errors of finite values are discussed in the text, that were constrained during fits of spectral data.

To fit 482 data, that model included 11 adjusted parameters; $U_{1,0}$, $U_{0,1}$, c_j with $1 \leq j \leq 6$, s_0^B , t_1^B and u_1^B ; we constrained values of t_0^B and t_0^F to be consistent with calculated values of electric dipolar moment and rotational g factor (S. P. A. Sauer and J. F. Ogilvie, to be published), in lieu of experimental values. The maximum range of validity of radial functions of BF in Table 3 is $1.10 \leq R/10^{-10} \text{ m} \leq 1.52$.

Data of AlF comprise 30 microwave transitions,^{19,22} employed in our previous analysis,²³ and 1076 vibration-rotational lines in the range up to $J = 102$ and $v = 9$;²¹ of the latter transitions, most had uncertainties set at 0.05 m^{-1} by the original authors.²¹ To fit these 1106 transitions required only eight independently adjustable parameters: $U_{1,0}$, $U_{0,1}$ and c_j with $1 \leq j \leq 6$, the same set previously fitted to fewer data;²³ we constrained values of t_0^A and t_0^F to conform with experimental values of electric dipolar moment²⁴ and rotational g factor²⁵ according to eqn. (9) and (10). Of the best fit, the normalised standard deviation is 1.00; the F statistic is 2.98×10^{14} . The maximum range of validity of radial functions of $^{27}\text{A}^{19}\text{F}$ in Table 3 is $1.43 \leq R/10^{-10} \text{ m} \leq 2.03$.

Data of InF include the same rotational²⁶ (19 in total, 16 for $^{115}\text{In}^{19}\text{F}$ up to $v = 3$ and $J = 19$ and three for $^{113}\text{In}^{19}\text{F}$ with $v = 0$ and up to $J = 18$) and vibration-rotational transitions²⁷ (475 lines of $^{115}\text{In}^{19}\text{F}$ up to $v = 9$ and $J = 102$ and 161 lines of $^{113}\text{In}^{19}\text{F}$ up to $v = 4$ and $J = 93$) treated in our previous analysis²⁸ supplemented by vibration-rotational transitions²⁹ of InF (2664 lines of $^{115}\text{In}^{19}\text{F}$ up to $v = 12$ and $J = 160$ and 179 lines of $^{113}\text{In}^{19}\text{F}$ up to $v = 3$ and $J = 106$); some lines were duplicated in the two sets of independent IR measurements. For vibration-rotational data in both sets,^{27,29} we fitted each band separately to band parameters to evaluate objectively the uncertainties and to identify outliers due to blended and overlapping spectral lines; for lines measured in emission²⁹ uncertainties were set in the ranges $0.063\text{--}0.097 \text{ m}^{-1}$ for $^{115}\text{In}^{19}\text{F}$ and $0.058\text{--}0.095 \text{ m}^{-1}$ for $^{113}\text{In}^{19}\text{F}$, whereas for lines measured in absorption²⁷ uncertainties were set in the range $0.05\text{--}0.07 \text{ m}^{-1}$ for $^{115}\text{In}^{19}\text{F}$ and at 0.07 m^{-1} for $^{113}\text{In}^{19}\text{F}$, except outliers of which the uncertainty was set sufficiently large that residuals failed to influence the quality of the fit. During our analysis we reassigned several lines near band heads that had been incorrectly assigned.²⁹ We reproduced these 3498 measurements with only eight independently adjusted parameters: $U_{1,0}$, $U_{0,1}$ and c_j with $1 \leq j \leq 6$, and with t_0^A and t_0^F constrained to the same values as in our previous analysis.²⁸ The normalised standard deviation of the best fit is 1.32; the F statistic is 2.33×10^{14} . The maximum range of validity of radial functions of InF in Table 3 is $1.75 \leq R/10^{-10} \text{ m} \leq 2.38$.

In Table 3 we provide a summary of results of all these new analyses of spectra of BF, AlF, GaF and InF for comparison with our previous results for TlF,²⁸ for which the maximum range of validity of radial functions is $1.85 \leq R/10^{-10} \text{ m} \leq 2.45$.

Discussion

In Table 3 we present the first comparison of radial coefficients and other properties of diatomic molecules that constitute a complete family within the periodic table of chemical elements, namely all known diatomic fluorides of elements of Group 13. Although the extent of spectra vary, from a maximum value of vibrational quantum number only $v = 5$ for BF to $v = 12$ for InF, our treatment of these spectra is as uniform as is practicable. In particular, we apply in all cases information on the electric dipolar moment and the rotational g factor (whether derived experimentally or

computationally). Of InF a value of g_J is available from neither source,²⁸ but the consistency of t_0^F within the series AlF, GaF and TlF leaves little doubt that t_0^F of InF differs insignificantly from 1.00; then the reported electric dipolar moment enabled an estimate of t_0^A . Values of equilibrium internuclear distances R_e [calculated from the directly evaluated parameter $U_{0,1} = h/(8\pi^2 c R_e^2)$ with h , Planck's constant and c the velocity of light *in vacuo*] of members of this family thus assume maximum physical significance, because in a systematic manner all known dependence on isotopic mass is eliminated as far as terms of the order of κ^6 : defined conventionally as the fourth root of the ratio of electronic and a nuclear mass, κ is the expansion parameter in the development of adiabatic and non-adiabatic terms relative to adjacent terms in the Hamiltonian [eqn. (1)].^{3,4} These distances, R_e , increase monotonically with increasing atomic number of the partner of the fluorine atomic centre. Likewise monotonically in the same order, c_0 [calculated as $U_{1,0}^2/(4U_{0,1})$] and k_e [from $U_{1,0} = k_e^{1/2}/(2\pi c)$] decrease, but c_4 increases. As data of GaF and TlF are relatively few (limited by spectral ranges of available laser diodes), c_5 and c_6 are poorly defined for these molecules; trends of these parameters are obscure. In contrast the magnitudes of c_1 , c_2 and c_3 increase monotonically from BF to InF but revert slightly for TlF; as these values are in all cases significantly evaluated, this effect seems to be no artifact.

Comparison of our results with those of other workers is appropriate. For GaF and TlF, no other authors analysed extensive IR spectra at the great resolution of our experiments. For AlF we include microwave data, specifically seven rotational transitions,²² omitted from a previous analysis.²¹ The accuracy of some data²² included in that analysis²¹ was questioned,¹⁹ but we found no extraordinarily large residuals from the suspect data. In our analysis of InF we included data of $^{113}\text{In}^{19}\text{F}$ for $v > 3$ that were omitted from a separate analysis.²⁹ Although Tiemann *et al.* originated this approach in their analysis of only pure rotational transitions that omitted non-adiabatic vibrational effects,³⁰ other workers routinely neglect information about the rotational g factor and electric dipolar moment that we apply to form t_0^A and t_0^F ; thus we ensure maximum significance of values of R_e by taking into account all these non-adiabatic effects. Our parameters in Table 3, that have mostly the form of radial coefficients, are an economical means (only 10–13 parameters in total, two constrained in each case) to reproduce 256–3498 precisely measured frequencies and wavenumbers of multiple isotopic variants (except AlF) essentially within their uncertainties. To regenerate these wavenumbers requires only simple analytic relations^{2,31} between radial coefficients and term coefficients Y_{kl} and various Z_{kl} that appear in an expression [eqn. (7)] of a type commonly used to form vibration-rotational terms,² of which the differences correspond to wavenumbers of transitions. According to our approach no repetitive and protracted numerical solution of a Schrödinger equation is needed to reproduce these wavenumbers, or (cautiously) to predict further transitions beyond the range of measurements included in our treatment. That such predictions served satisfactorily to assign lines of GaF beyond $v = 2$ demonstrates our approach to be efficient for that purpose.

Extra parameters, not uniformly required of molecules in this series, are u_1^{Tl} of TlF and s_0^B , t_1^B and u_1^B of BF. As explained previously,²⁸ u_1^{Tl} represents not truly adiabatic effects, which pertain to the finite mass of nuclides ^{203}Tl and ^{205}Tl , but an effect of their finite and isotopically varying volumes.³² When, during fits of spectra of BF, we constrained values of t_0^A and t_0^F as specified in Table 3, a marginally significant value of u_1^B was evaluated when that parameter was left freely adjustable; the quality of the fit improved when s_0^B

rather than u_1^B was adjusted, and this value of s_0^B was highly significant. t_1^B proved only marginally significant, but the F statistic was enhanced when this parameter was added to the model. Thus we conclude that truly adiabatic effects are undetectable with respect to the precision of existing measurements of frequencies and wavenumbers of transitions for molecules here other than BF.

In constraining according to eqn. (9) and (10) our values of t_0^M and t_0^F to use in the program RADIATOM,² we must distinguish which atomic centre is the negative pole of the electric dipole. Since for no fluoride species in this family is this information directly available from experiment, in the conventional sense that the rotational g factor is measured for more than one isotopic variant, we assumed the fluorine atomic centre of AlF, GaF, InF and TlF to constitute the negative pole of each dipole. Although the electric dipolar moment of AlF has only a moderate magnitude, the ratio $|\mu_e/(eR_e)|$ increases monotonically from 0.19 to 0.42 within the series from AlF to TlF. Not only would chemists tend to assume such a sense of polarity $^+MF^-$ for these four molecules, but also for AlF a rigorous calculation of electronic structure yielded that result.³³ Chemists might naively expect the sense of the polarity of BF (at the equilibrium internuclear distance R_e) to be analogously $^+BF^-$, although many calculations indicate the opposite result. A measurement of electric dipolar moment of BF yielded only a moderate magnitude of poor precision, $(1.7 \pm 0.7) \times 10^{-30}$ C m.³⁴ Most calculations indicate a magnitude generally about 2.7×10^{-30} C m or larger,³³ although the sense of polarity can depend on both the quality of the basis set and the extent to which electronic correlation is taken into account. Such calculations under the most refined conditions generally indicate the polarity $^-BF^+$. For two other diatomic molecules GeS (J. F. Ogilvie, to be published) and BrCl³⁵ that have sufficient isotopic variants, analyses of vibration-rotational spectra yielded not only magnitudes of both the electric dipolar moment and the rotational g factor but also their signs with respect to the nuclear framework; we achieved these results by freely fitting t_0^S and t_0^B from spectra (only wavenumbers of transitions, neither intensities nor shifts of frequencies from the Stark and Zeeman effects) and reverting eqn. (9) and (10) to deduce the corresponding values of μ_e and g_J .¹⁷ This approach is formally inapplicable to molecules in the present family because spectra are available for only variants containing ¹⁹F. To test whether a direct estimate of t_0^B is practicable, we fitted data of BF with a model consisting of parameters $U_{1,0}$, $U_{0,1}$, c_j with $1 \leq j \leq 6$, s_0^B , t_0^B and t_1^B , with t_0^F constrained to either zero or -1.3 ; in each case the converged value of t_0^B was -1.7 ± 0.04 , thus highly significant. That this magnitude exceeds that of the constrained value in Table 3 likely indicates neglect of adiabatic effects in the model, but inclusion of u_1^B in this fitting model hindered convergence. For electric polarity in the sense $^+BF^-$ the value of t_0^B is expected to be about -1.3 if g_J has a value about -0.20 ; t_0^B is insensitive to moderate variation of μ_e as thereby the first term within parentheses in eqn. (9) or (10) dominates. We may thus have discovered the first experimental evidence of the sense $^-BF^+$ of electric polarity of this diatomic species, in agreement with results of accurate calculations.³³

Conclusion

In a consistent and systematic manner we analysed all available data of frequencies of pure rotational transitions and wavenumbers of vibration-rotational transitions of all diatomic fluorides of elements in Group 13 of the periodic table: BF, AlF, GaF, InF and TlF in their electronic ground

states $X^1\Sigma^+$ or $X0^+$. On imposing information about the electric dipolar moment and the rotational g factor, we generated values of coefficients of radial functions, defined with respect to the Hamiltonian in eqn. (1); these coefficients constitute both the most compact and most chemically and physically meaningful parameters³⁶ that enable wavenumbers of spectral lines to be reproduced within essentially the great precision of their measurements: $|\delta\tilde{\nu}/\tilde{\nu}|$ of most lines is less than 10^{-6} . Characteristic parameters in Table 3 of molecules within this family exhibit regular trends.

J.F.O. thanks Professor P. F. Bernath for providing data of BF, AlF and InF and the National Science Council of the Republic of China for support. H.U. thanks Dr. J. W. C. Johns for providing spectral data of SO₂ for purposes of calibration.

References

- 1 D. E. Mann, B. A. Thrush, D. R. Lide, J. J. Ball and N. Acquista, *J. Chem. Phys.*, 1961, **34**, 420.
- 2 J. F. Ogilvie, *J. Phys. B*, 1994, **27**, 47.
- 3 F. M. Fernandez, *Phys. Rev. A*, 1994, **50**, 2953.
- 4 F. M. Fernandez and J. F. Ogilvie, *Chin. J. Phys.*, 1992, **30**, 177; 599.
- 5 H. Uehara, K. Horiai, Y. Ozaki and T. Konno, *Spectrochim. Acta, Part A*, 1994, **50**, 1389.
- 6 H. Uehara, K. Horiai, Y. Ozaki and T. Konno, *Chem. Phys. Lett.*, 1993, **215**, 505.
- 7 H. Uehara, K. Horiai, Y. Ozaki and T. Konno, *J. Mol. Struct.*, 1995, in the press.
- 8 G. Guelachvili and K. N. Rao, *Handbook of Infrared Standards*, Academic, New York, 1986.
- 9 J. Hoelt and K. P. R. Nair, *Chem. Phys. Lett.*, 1993, **215**, 371.
- 10 H. Uehara, K. Horiai, K. Nakagawa and H. Suguro, *Chem. Phys. Lett.*, 1991, **178**, 553.
- 11 J. F. Ogilvie, *Proc. R. Soc. London, Ser. A*, 1981, **378**, 287; 1982, **381**, 479.
- 12 J. F. Ogilvie, *J. Chem. Phys.*, 1988, **88**, 2804.
- 13 E. R. Cohen and P. Giacomo, *Physica A*, 1987, **146**, 1.
- 14 J. F. Ogilvie, *Ber. Bunsen-Ges. Phys. Chem.*, 1995, **99**, in the press.
- 15 A. H. Wapstra and G. Audi, *Nucl. Phys., A*, 1985, **432**, 1.
- 16 W. Gordy and R. L. Cook, *Microwave Molecular Spectra*, Wiley, New York, 1985, ch. 4 and 11.
- 17 J. F. Ogilvie and S. C. Liao, *Chem. Phys. Lett.*, 1994, **226**, 281.
- 18 A. H. M. Ross, R. S. Eng and H. Kildal, *Opt. Commun.*, 1974, **12**, 433.
- 19 J. Hoelt, F. J. Lvas, E. Tiemann and T. Torring, *Z. Naturforsch., A*, 1970, **25**, 1029.
- 20 R. Honerjager and R. Tischer, *Z. Naturforsch., A*, 1974, **29**, 1919.
- 21 K.-Q. Zhang, B. Guo, V. Braun, M. Dulick and P. F. Bernath, *J. Mol. Spectrosc.*, 1995, **170**, 82, and references therein.
- 22 F. C. Wyse, W. Gordy and E. F. Pearson, *J. Chem. Phys.*, 1970, **52**, 3887.
- 23 J. F. Ogilvie and S. F. Chuang, *J. Mol. Spectrosc.*, 1992, **154**, 1.
- 24 D. R. Lide, *J. Chem. Phys.*, 1965, **42**, 1013.
- 25 R. Honerjager and R. Tischer, *Z. Naturforsch., A*, 1974, **29**, 342.
- 26 J. Hoelt and K. P. R. Nair, *Z. Phys., D*, 1994, **29**, 203.
- 27 Y. Ozaki, K. Horiai, K. Nakagawa and H. Uehara, *J. Mol. Spectrosc.*, 1993, **158**, 363.
- 28 J. F. Ogilvie, S. C. Liao, H. Uehara and K. Horiai, *Can. J. Phys.*, 1994, **72**, 930.
- 29 T. Karkanis, M. Dulick, Z. Morbi, J. B. White and P. F. Bernath, *Can. J. Phys.*, 1994, **72**, 1213.
- 30 E. Tiemann, H. Arnst, W. U. Stieda, T. Torring and J. Hoelt, *Chem. Phys.*, 1982, **67**, 133.
- 31 J. F. Ogilvie, *Comput. Phys. Commun.*, 1983, **30**, 101.
- 32 J. Schlembach and E. Tiemann, *Chem. Phys.*, 1982, **68**, 21.
- 33 S. Huzinaga, E. Miyoshi and M. Sekiya, *J. Comput. Chem.*, 1993, **14**, 1440.
- 34 F. J. Lovas and D. R. Johnson, *J. Chem. Phys.*, 1971, **55**, 40.
- 35 J. F. Ogilvie, *J. Chem. Soc., Faraday Trans.*, 1995, **91**, 3005.
- 36 J. F. Ogilvie, *Spectrochim. Acta, Part A*, 1990, **46**, 43.